Complex monolithic and InP hybrid integration on high bandwidth electro-optic polymer platform

P. Groumas,[1,2] Z. Zhang[2], V. Katopodis,[1,*] Ch. Kouloumentas,[1] D. de Felipe,[2] R. Dinu,[3] E. Miller,[3] J. Mallari,[3] G. Cangini,[3] N. Keil,[2] H. Avramopoulos[1], and N. Grote[2]

[1]*School of Electrical and Computer Engineering, National Technical University of Athens, Zografou 15573, Athens, Greece*
[2]*Fraunhofer Institute for Telecommunications, HHI, Berlin 10587, Germany*
[3]*GigOptix Inc.19910 North Creek Parkway Suite 100, Bothell, WA, 98011, USA*
**Corresponding author: vkat@mail.ntua.gr*

Received May 31, 2012; revised Month X, XXXX; accepted Month X, XXXX;
posted Month X, XXXX (Doc. ID XXXXX); published Month X, XXXX

We report on the monolithic integration of multi-mode interference couplers, Bragg-gratings and delay-line interferometers on an electro-optic polymer platform capable of modulation directly at 100 Gb/s. We also report on the hybrid integration of InP active components with the polymer structure using the butt-coupling technique. Combining the passive and the active components, we demonstrate a polymer-based, external cavity laser with 17 nm tuning range and the optical assembly of an integrated 100 Gb/s transmitter, and we reveal the potential of the electro-optic polymer technology to provide the next generation integration platform for complex, ultra high-speed optical transceivers. © 2012 Optical Society of America
OCIS Codes: 130.5460, 140.3600, 230.2090, 230.3120,

New applications continue to emerge increasing the required bandwidth in every part of communication networks and demanding new generations of compact, ultra-fast optical transceivers. At the transmitter side, optical polymers appear as one of the most promising technologies, as they can possess extremely high electro-optic (EO) coefficients and can in principle provide bandwidth up to 200 GHz [1], thus having the potential to form the basis of transmitters for 100 Gb/s, and beyond.

Polymer modulators with record bandwidth in excess of 65 GHz are available today [2], but they come only as bulk devices in the same way as $LiNbO_3$ modulators do. This has as a consequence higher cost and limitations in their compactness, the range of functionalities they can support and their applicability in complex optical circuitry. To become cost effective and overcome these limitations, the EO polymer technology should mature and evolve from a device specific technology into a general purpose platform for photonic integrated circuits (PICs), in the same way as InP or silicon-on-insulator (SOI) technologies have evolved in the past [3-4]. This evolution has as a prerequisite the possibility to design and monolithically integrate complex passive structures with modulators on polymer boards using a single-fabrication step. Moreover, since practical polymer lasers and detectors are not available yet, it also prerequisites the possibility to hybridly integrate active components with the polymer boards.

In the present work, we move along this direction and reveal the potential of EO polymers to serve as a novel photonic integration platform. We present the design and fabrication of multi-mode interference (MMI) couplers, Bragg-gratings (BGs) and delay-line interferometers (DLIs), and we report on the hybrid integration of InP gain chips and distributed-feedback (DFB) lasers with polymer boards. Combining passive and active structures, we demonstrate the first EO polymer BG-based tunable laser and the optical assembly of a 100 Gb/s transmitter. Finally, we outline future plans for advanced transmitters based on the integration of the structures mentioned above with arrayed polymer modulators.

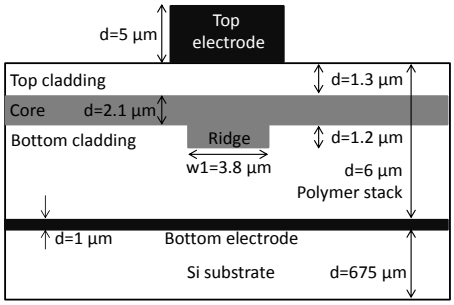

Fig. 1. Structure of EO polymer platform used in this work.

Fig. 1 depicts the cross-section of the single-mode polymer waveguide used in this work. The refractive indices of the core layer, the top cladding and the bottom cladding are 1.743, 1.388 and 1.505, respectively. The effective index of the ridge waveguide is 1.6603, and the mode-field diameter is 2.8 µm in the vertical and 4.6 µm in the lateral direction. The strong field confinement in combination with the high EO coefficient that the polymer material of the core features once poled (65 pm/V at 1550 nm) allows for strong EO effect and efficient modulation. The bottom electrode is part of the platform, whereas the top electrode is placed only above the active regions of the Mach-Zehnder modulators (MZM) to selectively pole these regions during material curing. The propagation loss of the waveguide is 1 dB/cm in the 1550 nm range.

Single Y-splitters or groups of Y-splitters in tree-like configurations are commonly used in PICs for power splitting due to their simple design. However, in order to reduce scattering loss, avoid multi-mode behavior and suppress back-reflection, long device lengths in excess of 500 µm are often required for the basic unit. The use of compact MMI structures in place of Y-splitters is thus highly desirable, especially with increasing splitting ratio and count of output ports. In this work, 1x2 and 1x4 MMI couplers were designed using the 3-dimensional beam

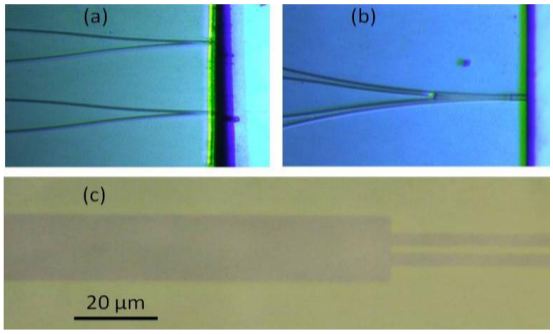

Fig. 2. Photographs of: (a) two 1x2 MMI couplers, and (b) a 1x4 MMI coupler. (c) Closer view on a 1x2 coupler with 12 μm width.

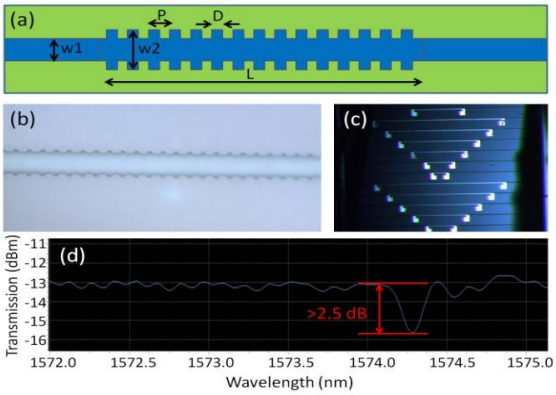

Fig. 3. (a) Design parameters of BGs, (b) fabricated BG structure, (c) polymer BG chip, (d) BG transfer function (dip at 1574.3 nm).

propagation method (3D-BPM) on the structure of Fig. 1, and were fabricated. Fig. 2a and 2b present images of polymer chips with 1x2 and 1x4 MMI couplers. A closer view on a 1x2 coupler is shown in Fig. 2c. To compensate for material index uncertainties and fabrication imperfections, each optimal design was expanded to a design parameter variation set on the mask. The testing of the components revealed that the optimum width and length of the multi-mode region was 12 μm and 136 μm for the 1x2 couplers and 28 μm and 241 μm for the 1x4 couplers, respectively. For these values, the insertion loss remained lower than 0.8 dB and the power imbalance at the output ports lower than 0.2 dB in both cases. Good design to fabrication integrity was confirmed by the small variation between simulation and experimental results.

BGs are structures that represent a periodic or quasi-periodic perturbation of the effective refractive index of a waveguide and act as optical filters. An efficient way to realize a BG in the waveguide of Fig. 1 involves the perturbation of the width of the ridge in the core layer and the generation of a "side grating" layout, as shown in Fig. 3a. To overcome limitations in the fabrication resolution that are associated with the conventional i-line photo-lithography used for wafer-scale production, 5th order designs were adopted according to the relationship [5]:

$$m\,\lambda_B = 2 \cdot n_e \cdot \Lambda \qquad (1)$$

where m the diffraction order, λ_B the Bragg wavelength, n_e the effective mode index and Λ the period of the grating. To set the λ_B in the vicinity of 1550 nm, a grating period of 2.343 μm was chosen, while the number of periods and the strength of the grating perturbations served as additional design parameters in order to achieve

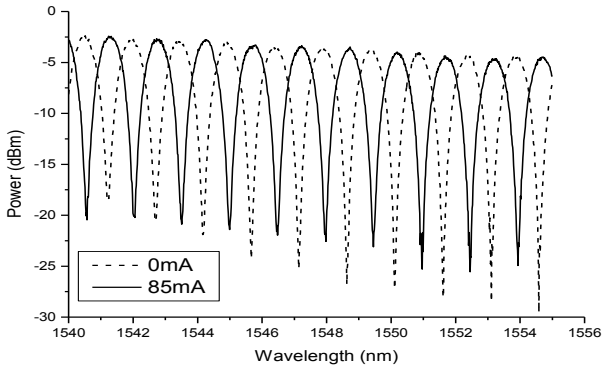

Fig. 4. Transfer function of 160 GHz DI with full π-shift capability by injecting current into the thermal phase-shifter.

high reflectivity at reasonable device length [6]. Fig. 3b presents a microscope image of the core layer during an intermediate step of the fabrication. Fig. 3c depicts in turn the final polymer chip with BGs of variable lengths. As observed, metal electrodes were placed on the top layer of this chip to run along the BGs and provide a means for tuning the λ_B via the thermo-optic effect on the polymer material. Despite the limited fabrication resolution, efficient operation could be recorded for BGs with a large number of periods (i.e. 800 periods or 1874.4 μm length) and hard perturbation designs (i.e. w1=3.8 μm and w2=6.3 μm). As shown in Fig. 3d, for these values, a clear dip appears in the experimental reflection spectrum of the BG. The filter effect is 2.5 dB, which corresponds to ~40% reflectivity. It is noted that although lower than the value predicted by simulations, this reflectivity is absolutely sufficient to support lasing within typical laser cavities.

Finally, DLIs are realized in PICs as unbalanced Mach-Zehnder interferometers. Apart from providing a means for optical filtering in the circuit, the DLIs can enable other functionalities such as decoding of phase modulated signals [7] and format conversion [8]. Two DLI designs with 160 and 200 GHz free spectral range (FSR) were fabricated on the polymer platform. Metal electrodes were added on the top to act as thermal phase-shifters. Fig. 4 presents the transmission spectra of the 160 GHz DLI for 0 and 85 mA current at the phase-shifter and reveals that the complete π phase-shift is obtained. The length of the 160 GHz device is 12.95 mm, the insertion loss below 6 dB, the polarization dependent loss below 0.3 dB and the extinction-ratio higher than 17 dB.

As a first step for the hybrid integration of active components, an InP gain chip with a single reflector was butt-coupled to the chip of the polymer BG described above. The BG with 40% reflectivity can serve as a semi-transparent mirror, and thus the hybrid assembly can act as an external-cavity laser with the cavity extending both over the InP and the EO polymer sections. Fig. 5a illustrates the laser assembly operating in transverse electrical (TE) polarization. The coupling loss at the InP/polymer interface is approximately 2 dB due to the imperfect overlap between the mode profiles of the InP and the polymer waveguides. The gain chip can compensate, however, for this loss, and can provide a net gain inside the cavity. Wide tunability of the emission wavelength in excess of 17 nm is achieved by thermally shifting the BG reflection peak, as shown in Fig. 5b. The

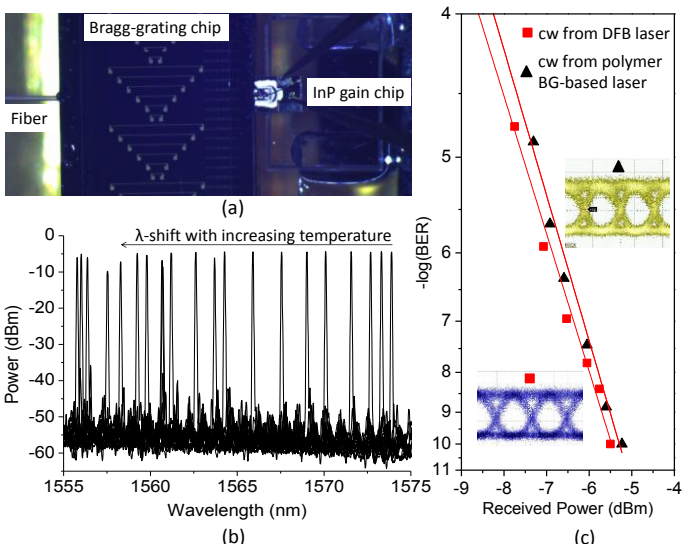

Fig. 5. (a) Photograph of the polymer BG-based laser, (b) shift of the emission wavelength with temperature, and (c) BER curves of 40 Gb/s modulated signals using as input cw the output of the polymer BG-based laser or the output of a DFB laser at 1566 nm. Indicative eye-diagrams for the two cases are shown in the insets.

thermo-optic coefficient of the polymer material is $-1.4 \cdot 10^{-4}$ 1/°C, while the heating power required to cover the 17 nm range is 800 mW. However, optimization of the electrode design in terms of size, position, thickness and material is expected to reduce this power by at least a factor of 2. The line-width of the continuous wave (cw) laser output was measured using homodyne and intradyne methods and found below 1.5 MHz within the available tuning range. The laser line-width can be further reduced by limiting the spectral width of the grating filter. Finally, the laser output at variable wavelengths was amplitude modulated using a conventional $LiNbO_3$ modulator at 40 Gb/s and was compared against the modulated cw from typical DFB lasers at the same wavelengths. Fig. 5c presents indicative results from this comparison at 1566 nm, and reveals through bit-error rate (BER) curves and eye-diagrams the effectiveness of the polymer BG-based laser.

As a second step, a novel 100 Gb/s transmitter was developed involving the hybrid integration of a DFB laser with an ultra-fast polymer MZM [2]. Due to the molecular properties of the system of Fig. 1, the electro-optic effect is present in the core only for transverse magnetic (TM) modes. As, however, the DFB laser was designed to provide TE modes, it was necessary to rotate the polarization of the laser output either with a half-wave plate before the polymer board or by flipping the laser by 90°. Fig. 6 depicts the optical assembly of the transmitter using the second option. The loss at the InP/polymer interface was 2.2 dB, which was close to the corresponding value for the TE modes, as the laser had a rather circular mode profile. The laser spectrum at the output of the assembly is shown in Fig. 7. The low power indicates high loss inside the MZM, which is explained by the absence of any bias current, and thus by that the MZM was not at its transmission peak. Integration of the optical assembly with a bias circuit and high-speed InP electronics [9] will follow and will be reported in a future work.

In conclusion, we have presented monolithic integration

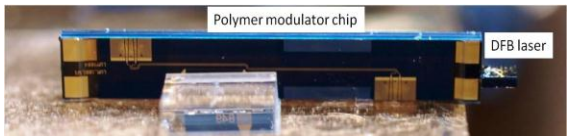

Fig. 6. Optical assembly of the 100 Gb/s transmitter.

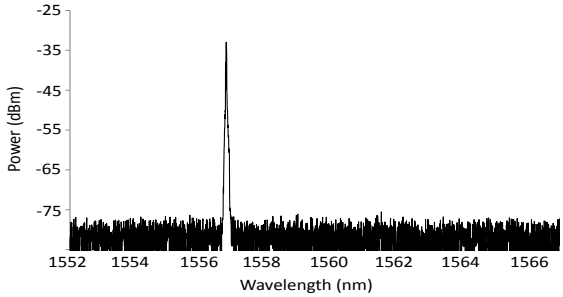

Fig. 7. Spectrum at the MZM output at 50 mA driving current.

of advanced passive structures on an EO polymer platform. These structures include 1x2 and 1x4 MMI couplers with 0.8 dB insertion loss and 0.2 dB power-imbalance, 5th order tunable BGs with up to 40% reflectivity and DLIs with complete π-shift capability. We have also reported on the hybrid integration of InP gain chips and DFB lasers with the EO polymer chips based on butt-coupling. Using these structures we have demonstrated an external cavity laser with 17 nm tunability and the optical assembly of a novel 100 Gb/s transmitter, unveiling the potential of the EO polymer technology to provide the next generation integration platform for ultra-fast optical transceivers. Next steps involve further combination of passive and active structures with single and arrayed polymer modulators for tunable 100, 2x100 and 4x100 Gb/s transmitters and integrated optical interconnects.

The work was supported by the European Commission funded project ICT-POLYSYS (Contr. No. 258846).

References

1. M. Lee, H. E. Katz, C. Erben, D. M. Gill, P. Gopalan, J. D. Heber, D. J. McGee, Science **298**, 1401 (2002).
2. J. Mallari, C. Wei, D. Jin, G. Yu, A. Barklund, E. Miller, P. O'Mathuna, R. Dinu, A. Motafakker-Fard, B. Jalali, in OFC Conference, San Diego USA, March 2010, OThU2.
3. R. Nagarajan, M. Kato, J. Pleumeekers, P. Evans, S. Corzine, S. Hurtt, A. Dentai, S. Murthy, M. Missey, R. Muthiah, R.A. Salvatore, C. Joyner, R. Scneider, M. Ziari, F. Kish, and D. Welch, IEEE J. Select. Top. Quantum Electron. **16**, 1113 (2007).
4. B. Jalali, Nat. Photon. **1**, 193 (2007).
5. S.J. Mihailov, M.C. Gower, Electron. Lett. **30**, 707 (1994).
6. A. Yariv and M. Nakamura, J. Quantum Electron. **V. QE-13**, no 4, pp. 233-253, April 1977.
7. M. Bougioukos, T. Richter, Ch. Kouloumentas, V. Katopodis, R. Harmon, D. Rogers, J. Harrison, A. Poustie, G. Maxwell, C. Schubert, and H. Avramopoulos, IEEE Photon. Technol. Lett. **23**, 1649 (2011).
8. P. Groumas, V. Katopodis, Ch. Kouloumentas, M. Bougioukos, and H. Avramopoulos, IEEE Photon. Technol. Lett. **24**, 179 (2012).
9. J.-Y. Dupuy, A. Konczykowska, F. Jorge, M. Riet, P. Berdaquer, J. Moulu, J. Godin, Electron. Lett. **46**, 55 (2010).

Full References

1. M. Lee, H. E. Katz, C. Erben, D. M. Gill, P. Gopalan, J. D. Heber, D. J. McGee, "Broadband Modulation of Light by using an Electro-Optic Polymer," Science **298**, 5597, pp. 1401-1403, November 2002.
2. J. Mallari, C. Wei, D. Jin, G. Yu, A. Barklund, E. Miller, P. O'Mathuna, R. Dinu, A. Motafakker-Fard, B. Jalali, "100Gbps EO Polymer Modulator Product and Its Characterization using a Real-Time Digitizer," in Optical Fiber Communications (OFC) Conference, San Diego, California, USA, paper OThU2, March 21-25, 2010.
3. R. Nagarajan, M. Kato, J. Pleumeekers, P. Evans, S. Corzine, S. Hurtt, A. Dentai, S. Murthy, M. Missey, R. Muthiah, R.A. Salvatore, C. Joyner, R. Scneider, M. Ziari, F. Kish, and D. Welch, "InP Photonic Integrated Circuits," IEEE Journal of Selected Topics in Quantum Electronics **16**, no. 15, pp. 1113-1125, September/October 2007.
4. B. Jalali, "Teaching silicon new tricks," Nature Photonics **1**, no. 4, pp. 193-195, April 2007.
5. S.J. Mihailov, M.C. Gower, "Recording of efficient high-order Bragg reflectors in optical fibres by mask image projection and single pulse exposure with an excimer laser," Electronics Letters **30**, no. 9, pp. 707-709, April 1994.
6. A. Yariv and M. Nakamura, "Periodic Structures for Integrated Optics," J. Quantum Electron. **V. QE-13**, no 4, pp. 233-253, April 1977.
7. M. Bougioukos, T. Richter, Ch. Kouloumentas, V. Katopodis, R. Harmon, D. Rogers, J. Harrison, A. Poustie, G. Maxwell, C. Schubert, and H. Avramopoulos, "Phase-Incoherent DQPSK Wavelength Conversion Using a Photonic Integrated Circuit," IEEE Photonics Technology Letters **23**, no. 22, pp. 1649-1651, November 2011.
8. P. Groumas, V. Katopodis, Ch. Kouloumentas, M. Bougioukos, and H. Avramopoulos, "All-Optical RZ-to-NRZ Conversion of Advanced Modulated Signals," IEEE Photonics Technology Letters **24**, no. 3, pp. 179-181, February 2012.
9. J.-Y. Dupuy, A. Konczykowska, F. Jorge, M. Riet, P. Berdaquer, J. Moulu, J. Godin, "Differential distributed amplifier with 2:1 selector in InP DHBT for 100 Gbit/s operation," Electronics Letters **46**, no. 1, pp. 55-57, January 2010.